Polymorphism of Dehydrobenzo[14]annulene Possessing Two Methyl Ester Groups in Noncentrosymmetric Positions

Ichiro Hisaki,*,[†] Eriko Kometani,[†] Hajime Shigemitsu,[†] Akinori Saeki,[‡,§] Shu Seki,[‡] Norimitsu Tohnai,[†,§] and Mikiji Miyata*,[†]

[†]Department of Material and Life Science, and [‡]Division of Applied Chemistry, Graduate School of Engineering, Osaka University, Suita, Osaka 565-0871, Japan

[§]PRESTO Japan Science and Technology Agency (JST), Japan

Ⓢ *Supporting Information*

ABSTRACT: We revealed that the π-conjugated cyclic compound octadehydrotribenzo[14]annulene ([14]DBA), with two methyl ester groups in noncentrosymmetric positions, formed five polymorphic crystals: forms I (plate, $P2_1/c$), II (block, $P2_1/c$), II' (block $P\bar{1}$), III (needle, $P2_1/c$), and IV (needle, $C2/c$), which is the largest number for polymorphic crystals of the DBA family. Forms I, III, and IV can be obtained selectively upon the crystallization conditions applied. The present polymorphism was provided by conformational flexibility and varied CH/O interaction methods of the methyl ester groups. The thermal stability, fluorescence properties, and photoconductivity of the polymorphs were investigated. Such proper-

ties are affected by the polymorphic supramolecular structure. Furthermore, we demonstrate that the polymorphs exhibit physical or chemical defects depending on the magnitude of the π-overlap of the DBA planes and that the fluorescence and electronic properties are strongly affected by the defects. Particularly, form I shows a significant fluorescence band at 530 nm, probably due to defects in the crystals.
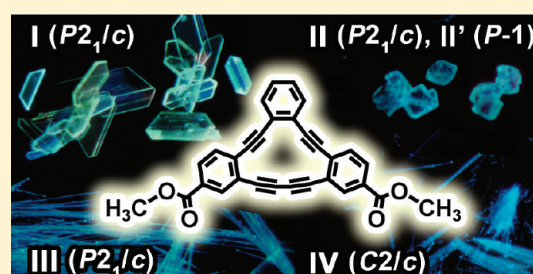
■ INTRODUCTION

The functionality of solid state materials based on π-conjugated molecules is crucially affected by their molecular arrangements.[1] Therefore, understanding of the relationships between structures and properties is significantly important. Polymorphic crystals[2] are exactly the appropriate systems to reveal the abovementioned relationships clearly because their varied supramolecular structures are just composed of a unique molecule or component. Indeed, a number of structure-dependent properties have been reported on the basis of polymorphs: those include conductivity,[2c,3] magnetic properties,[2c,4] solid state reactions,[2c,5] photochromism,[2c,6] and fluorescence emission.[2c,7]

As pointed out by McCrone, every compound essentially has the potential to give polymorphic crystals.[8,9] However, to obtain polymorphs more effectively, conformational flexibility and multifunctional groups providing versatile intermolecular interactions are generally required for molecules, i.e., conformational polymorphism (Figure 1a)[10] and synthon polymorphism (Figure 1b),[11] respectively. For example, Yu and co-workers revealed seven polymorphic crystal structures of the molecule so-called ROY, which are provided due to its versatile conformers,[12] and Nangia and co-workers reported 19 symmetry-independent conformers of 4,4-diphenyl-2,5-cyclohexadienone in its polymorphic crystals.[13] Co-crystals composed of multifunctionalized compounds also yield polymorphs frequently due to a heterosynthon, that is a hydrogen bonded recognition unit between dissimilar molecules.[14]

In this study, we planned to obtain polymorphs of π-conjugated molecules by taking advantage of the conformational and interactional flexibility of methyl ester groups (Figure 1c). The intended polymorph preparation based on large planar π-conjugated molecules is still an important challenge,[15] because the consequent polymorphs were expected to show varied arrangements concerning π-overlap geometries and coplanarity of adjacent π-planes, which affect the optical and electrical properties of the bulks (Figure 1d).[16,17]

As a π-conjugated molecule to obtain polymorphs, we applied octadehydrotribenzo[14]annulene ([14]DBA).[18] The compound was first reported by Vollhardt, Youngs, and co-workers as a monomer of topochemical polymerization.[19] Haley and co-workers synthesized a number of its derivatives, such as a series of octadehydro[14]annulenes annelated by 0 to 3 benzene ring-(s)[20] and [14]annulene-based hybrid systems annelated by dihydropyrene[21] and paracyclophene,[22] to investigate a magnetic-induced ring current on the annulene rings. They also reported [14]DBA-based donor—acceptor systems[23] and expanded systems,[24] which show significant optical properties. However, systematical investigation of [14]DBA-based supramolecular structures in the solid state has not been reported.
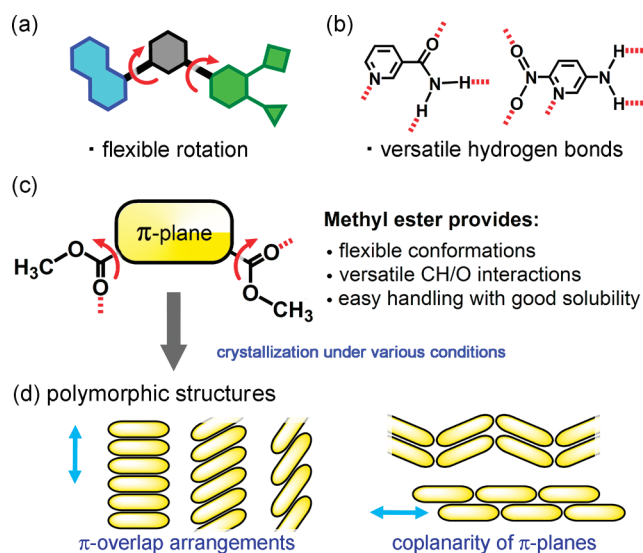
Figure 1. Schematic representation of strategies for affirmative emergence of polymorphs: conventional systems with (a) conformational flexibility and (b) multifunctional groups and (c) the present system with methyl esters groups at noncentrosymmetric positions, which is expected to yield varied stacking geometries concerning π-overlap and coplanarity of adjacent π-planes (d).

**Scheme 1. Octadehydrotribenzo[14]annulene Derivative**
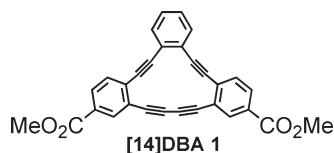
Therefore, construction of various molecular arrangements of [14]DBA in the solid state might lead to development of significant optical and electrical materials and topochemically polymerized functional materials.

Herein, we describe the preparation and crystallographic characterization of five polymorphs obtained from [14]DBA **1** with two methyl ester groups at the *syn*-positions (Scheme 1). The parent compound of **1** has just one crystalline form, while the five polymorphs are the largest numbers for polymorphic crystals in the DBA family.[19] This fact indicates that the noncentrosymmetric introduction of a methyl esters in conjugated planar molecules can be a useful strategy to obtain polymorphs affirmatively. Furthermore, the thermal stability, fluorescent, and electronic properties of the polymorphs were investigated. Such properties are dependent on the polymorphs. Interestingly, we revealed that the polymorphs exhibited structural defects depending on the degree of π-overlap of the DBA planes and that the fluorescence and electronic properties were strongly affected by the defects. Particularly, form I shows a significant fluorescence band at 530 nm, probably due to defects in the crystals.

■ RESULTS AND DISCUSSION

Molecular Design and Synthesis. Previously, we reported that the octadehydro[12]annulene derivative with methyl phthalate

Scheme 2. Conformational (a) and Interactional (b) Flexibility of [14]DBA 1 with Methyl Ester Groups[a]
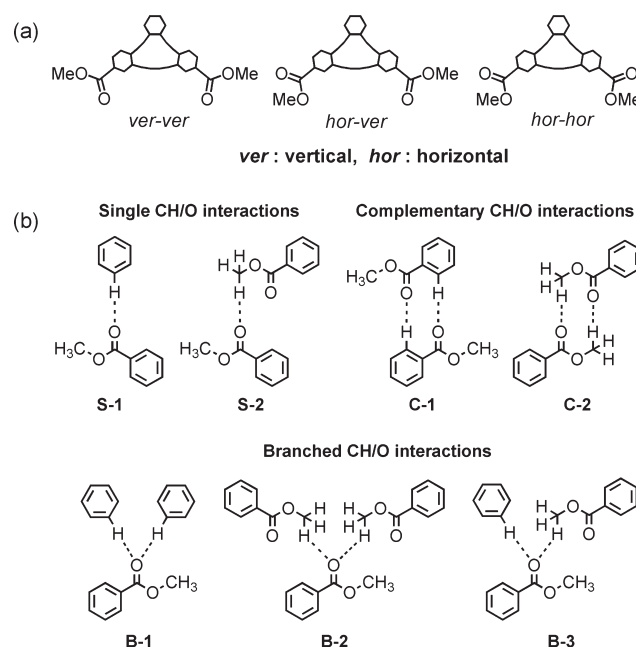

[a] Part a shows three conformers of **1**: the *ver-ver*, *hor-ver*, and *hor-hor* conformations, which are classified according to the direction (vertical or horizontal) of the carbonyl groups in the ester. Part b is a schematic representation of the versatile CH/O interactions expected for **1**: the single, complementary, and branched CH/O interactions.

moieties and the naphthalene derivative with two methyl ester groups yielded three and two polymorphs, respectively.[25] On the basis of these results, we propose an empirically derived hypothesis that noncentrosymmetric introduction of methyl ester groups into the periphery of a π-plane tends to provide polymorphs, due to the following aspects of the group: (1) Rotational flexibility of the methyl ester can provide conformers, i.e. the *ver-ver*, *hor-ver*, and *hor-hor* conformers (Scheme 2a), where *ver* and *hor* denote the vertical and horizontal direction of the carbonyl group, bringing about significant changes of the dipole and quadrupole moments of the molecule and electrostatic potential surface on the molecule.[25a] (2) The carbonyl oxygen atom in the group can involve weak, less directional, and, therefore, geometrically- and topologically versatile CH/O interactions[26] with electrostatically positive hydrogen atoms such as those of aromatic rings and methyl groups (Scheme 2b), allowing the π-conjugated core to pack into various arrangements. (3) The compounds functionalized by the group show better solubility for organic solvents than functional groups such as carboxylic acid and urea, allowing the compound to be subjected to various crystallization conditions, i.e., solvents and temperatures.

[14]DBA **1** was synthesized according to Scheme 3. Pd-catalyzed cross-coupling reaction of iodobenzene derivative **2**[17] and diethynylbenzene **3** gave acyclic tetrayne **4**. Desilylation followed by Cu-mediated oxidative intramolecular cyclization gave **1** in good yield.

Crystal Structures of Polymorphs. Crystallization under various conditions yielded totally five polymorphic crystals as shown in Figure 2: forms I (plate, $P2_1/c$), II (block, $P2_1/c$), II' (block $P\bar{1}$) III (needle, $P2_1/c$), and IV (needle, $C2/c$), where the crystal morphologies and the space groups are in parentheses.[27]

Scheme 3. Synthesis of [14]DBA 1[a]
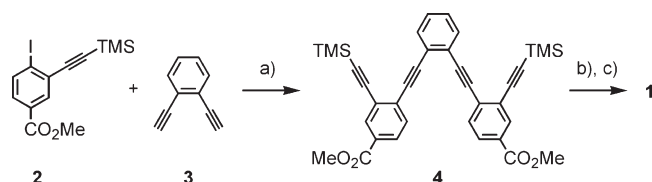
[a] Reagents and reaction conditions: (a) Pd(PPh$_3$)$_4$, CuI, *i*-Pr$_2$NH, THF, RT, 22 h, 78%; (b) TBAF, THF, RT, 1 h; (c) CuCl, pyridine, MeOH, RT, 2 h, 69% for 2 steps. TBAF, tetrabutylammonium fluoride; TMS, trimethylsilyl.
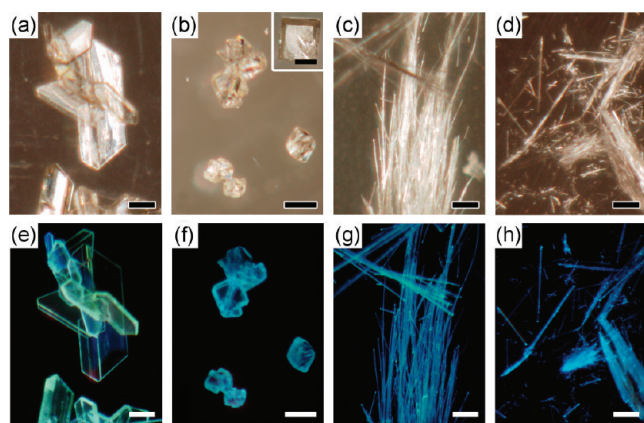

Figure 2. Photos of the polymorphs under ambient light (top) and UV light with wavelength of 365 nm (bottom): forms I (a, e), II and II′ (b, f), III (c, g), and IV (d, h). Scale bars: 200 μm. Forms II and II′ are obtained as a mixture, where a typical crystal shape of form II′ is cubic (inset), while that of form II shows an irregular mosaic morphology.

These crystals are generally obtained concomitantly and depending on the crystallization batches (Table S1). The appearance frequency of the forms is in the following order: I, III, II ∼ II′, IV. However, careful consideration of the crystallization conditions achieved almost selective formation of individual forms except for forms II and II′: form I was solely obtained by slow evaporation (SE) of ethyl acetate/dichloromethane solution at ambient temperature (AT). Form III was obtained by SE from tetrahydrofuran solution at AT. Sonication of the gelly materials obtained from SE of a toluene solution at −19 °C also gave crystalline bulk of form III. Form IV appeared only by cooling of supersaturated 1,2-dichloroethane solution at ca. −19 °C. A mixture of forms II and II′ (abbreviated as form II/II′) was formed by SE of a chloroform and 1-propanol solution at AT. However, despite many attempts, forms II and II′ were difficult to obtain separately. Structural uniformity of the obtained crystalline bulks was confirmed by consistency of the experimental and simulated powder X-ray diffraction patterns (see Figure S3).

Since the block crystals of form II exhibited high mosaicity and the needle crystals had width no more than 10 μm, determination of crystal structures was performed by synchrotron X-ray diffraction spectroscopy as well as with general equipment.[28] Figure 3 shows the crystal structures of the polymorphs with their hierarchical interpretation[29] in the following order: (i) molecular conformations, (ii) expediential dimeric motifs, (iii) the motif's arrangements, and (iv) crystal structures. [14]DBA 1 in forms I,

II, II′, and III exhibits the *ver-ver* conformation, while that in form IV exhibits the *hor-ver* conformation. No *hor-hor* conformation was observed in the present polymorphs, although the conformation was preliminarily observed in the solvate of 1 with 1,2,4-trichlorobenzene.

Because of the isosceles triangular shape of 1, the molecules in the each polymorph form parallelogram—dimeric pairs with the inversion center as expediential motifs of the crystals, where directional interaction was not necessarily observed in the motif. The dimeric motifs of forms I, II, and II′ have similar coplanar geometries, while those of forms III and IV have uneven parallel geometries, as shown in Figure 3(ii).

As shown in Figure 3a, the motif in form I is aligned one-dimensionally to form a tapelike structure. The tape is slipped-stacked to form a layer parallel to the *ab* plane. The adjacent layers (green and yellow ones) are staggered by 45.1°. Two types of CH/O interactions are observed among the layers; one is between the carbonyl and the methoxy group (type S1): C30-(A)−H⋯O3 (C⋯O distance, 3.14 Å; C−H−O angle, 111.2°); the other is a branched interaction involving the carbonyl, methoxy, and phenyl groups (type-B1): C28(B)−H⋯O1 (C⋯O distance, 3.33 Å; C−H−O angle, 122.5°) and C16-(C)−H⋯O1 (C⋯O distance, 3.51 Å; C−H−O angle, 143.8°).

In form II (Figure 3b), the dimeric motif aligns into an offset arrangement to form a planar sheet parallel to the (1 0 4) plane. The sheet is slipped-stacked to form a coplanar structure. [14]DBA 1 participates in two in-plane CH/O interactions between the carbonyl and phenyl groups (type S2): C17-(A)−H⋯O3 (C⋯O distance, 3.19 Å; C−H−O angle, 132.3°) and C15(B)−H⋯O1 (C⋯O distance, C⋯O distance, 3.60 Å; C−H−O angle, 178.6°).

Interestingly, a sheet motif of form II′ (Figure 3c) parallel to the (1 −1 6) plane is quite similar to that of form II. The CH/O interactions are also observed in similar way: C17(A)−H⋯O3 (C⋯O distance, 3.19 Å; C−H−O angle, 132.7°) and C15′−H⋯O1 (C⋯O distance, 3.65 Å; C−H−O angle, 176.0°).[30] The only significant difference between forms II and II′ is emerged in the stacking of the sheet motifs: their slipped-stacking directions are opposite, as shown by the blue arrows in Figure 3 (also see, Figure 4). Because of the slight difference, these two forms are difficult to obtain in complete solitude.

In form III (Figure 3d), 1 forms the slipped-stacked columnar assembly with large π-overlap along the *c* axis. The adjacent pairs colored in green and yellow are staggered by 50.7°, while those in the same color are parallel. Two types of CH/O interactions are observed: one is the B1-type branched interactions: C30-(A)−H⋯O3 (C⋯O distance, 3.52 Å; C−H−O angle, 162.4°) and C17(B)−H⋯O3 (C⋯O distance, 3.31 Å; C−H−O angle, 131.3°). The other is the self-complementary CH/O interaction involving the aromatic hydrogen atoms (type C-1): C7−H⋯O1(C) and C7(C)−H⋯O1 (C⋯O distance, 3.27 Å; C−H−O angle, 161.4°). Contrary to the *ver-ver* conformation in forms I−III, 1 in form IV exhibits the *hor-ver* conformation. As shown in Figure 3e, the carbonyl group with the horizontal conformation leads to a complementary CH/O interaction to form the uneven parallel dimeric motif: C29−H⋯O3(B) and C29(B)−H⋯O3 (C⋯O distance, 3.30 Å; C−H−O angle, 125.9°). The carbonyl oxygen O3 also contacts with a methoxy group to form a CH/O bond: C17-(C)−H⋯O3 (C⋯O distance, 3.39 Å; C−H−O angle, 140.8°). The carbonyl group with the vertical conformation

5490

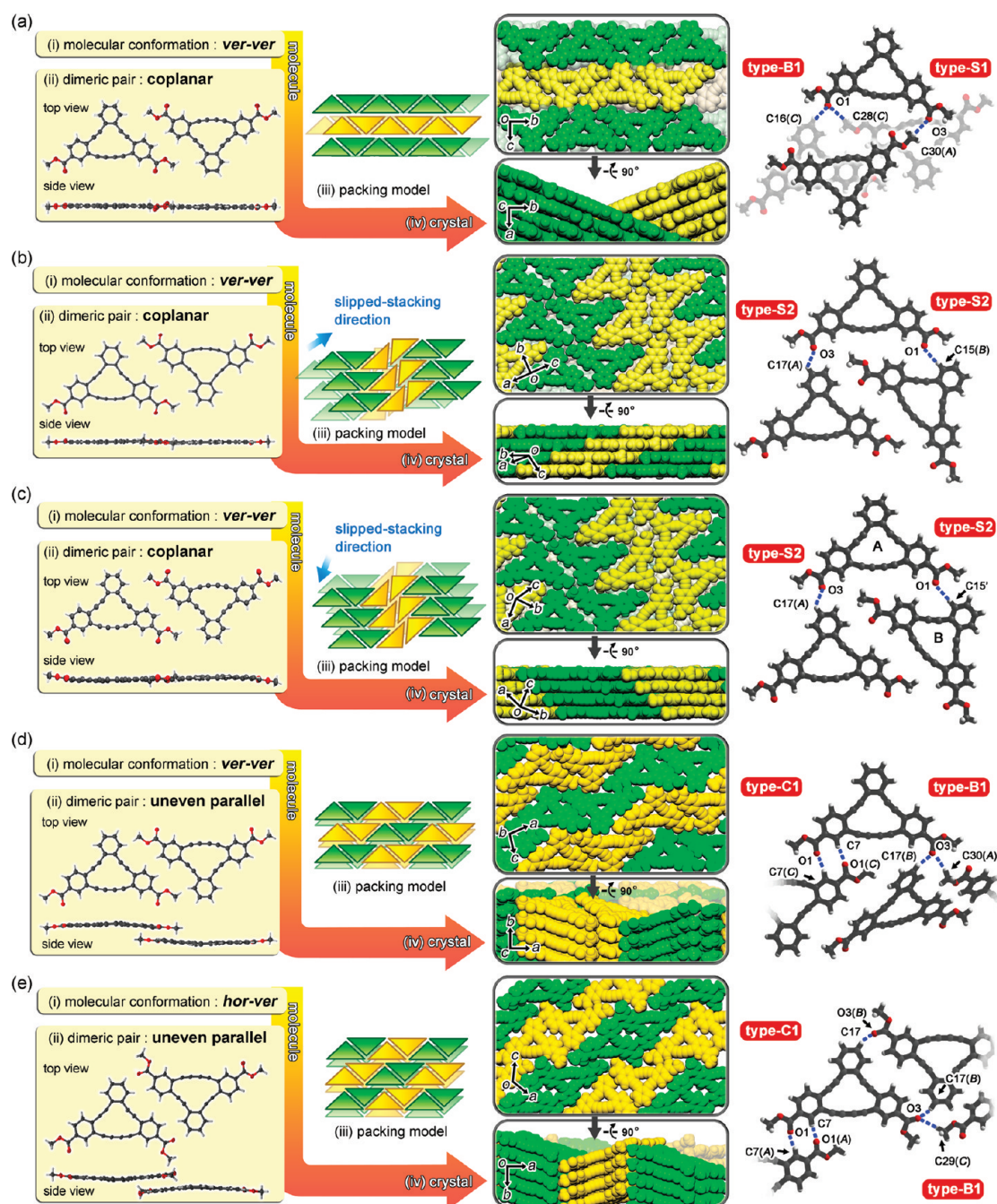dx.doi.org/10.1021/cg201075z |*Cryst. Growth Des.* 2011, 11, 5488–5497

Figure 3. Comparison of crystal structures of forms I (a), II (b), II′ (c), III (d), and IV (e) based on hierarchical interpretation in the following order: (i) molecular conformation, (ii) dimeric motif, (iii) the motif's arrangement, and (iv) crystallographic packing diagram. (Right column) CH/O interactions of the carbonyl oxygen atoms in the polymorphs. Totally, four kinds of CH/O interaction patterns (S-1, S-2, B-1, and C-1) were observed. The dimeric motifs of forms I, II, II′, and IV are described in thermal ellipsoids with 50% probability, while that of form III is drawn in ball-stick due to a problem of data quality. In the motif's arrangements, the molecules are schematically described with green and yellow isosceles triangles. The molecules in the packing diagrams are also colored yellow and green for clarity. Form II′ has two nonsymmetrical DBA molecules, A and B. Symmetry code for form I: (A) $1 - x, {}^1/_2 + y, {}^3/_2 - z$; (B) $2 - x, -{}^1/_2 + y, {}^3/_2 - z$; (C) $x, {}^5/_2 - y, {}^1/_2 + z$. For form II: (A) $x, 1 + y, z$; (B) $-x, {}^1/_2 + y, {}^3/_2 - z$. For form II′: (A) $-1 + x, -1 + y, z$. For form III: (A) $2 - x, {}^1/_2 + y, {}^3/_2 - z$; (B) $x, {}^3/_2 - y, {}^1/_2 + y$; (C) $1 - x, 1 - y, 1 - z$. For form IV: (A) ${}^1/_2 - x, {}^1/_2 - y, 1 - z$; (B) $1 - x, 1 - y, 2 - z$; (C) ${}^1/_2 + x, {}^1/_2 - y, {}^1/_2 + z$.

forms the C-1 type self-complement CH/O interaction: C17−H···O1(A) and C7(A)−H···O1 (C···O distance, 3.30 Å; C−H−O angle, 160.4°). The adjacent dimeric pairs colored in green and yellow are staggered by 51.0°. The molecules packed into a slipped-stacked columnar assembly with large π-overlap are similar to that of form III. Figure 4 shows two

layers of DBA molecules in the polymorphs. Forms III and IV exhibit larger overlaps of the DBA planes compared with forms I, II, and II′.

A carbonyl oxygen atom can accept one or two hydrogen atoms to make CH/O interactions. In the present systems, the carbonyl oxygen atoms participate totally in four types of CH/O
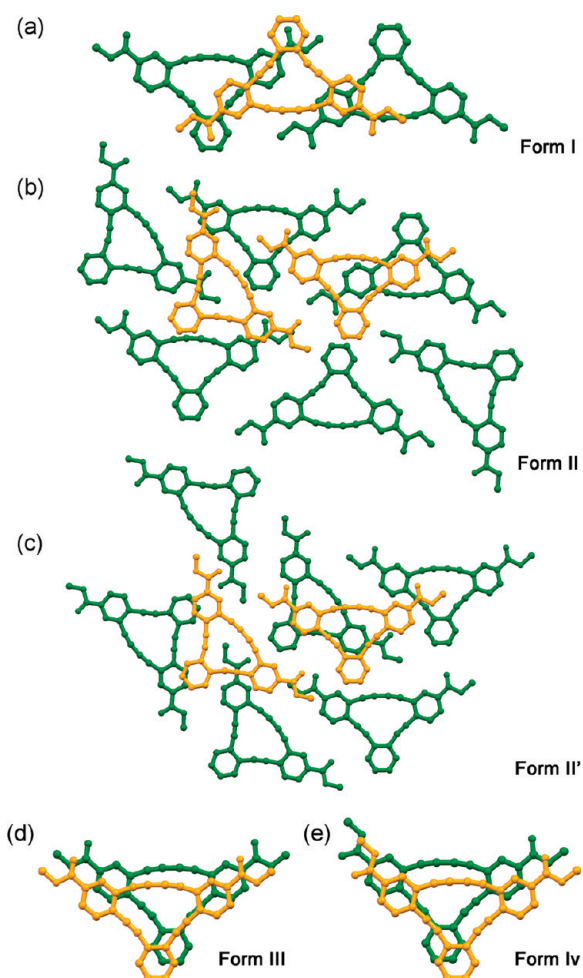
Figure 4. Stacking geometry of the DBA plans in the polymorphs. The selected packing diagrams are viewed from directly above the DBA planes.

Table 1. Geometric Parameters of [14]DBA in Crystalline States

form	$R_{1,4}$ (Å)	d (Å)	γ (deg)	T (°C)	$\Delta H°$ (kJ/mol)
1 (form I)	5.68	8.92	23.2	254 (dec)[c]	314
1 (form II)	7.20	10.13	31.3		
1 (form II′)[a]	6.87	9.88	29.5	252 (dec)[c,d]	359
	7.06	10.12	28.3		
1 (form III)	4.47	3.87	69.8	240 (dec)[c]	312
1 (form IV)	4.49	3.81	76.3	245 (dec)[c]	293
parent	3.92	6.31	35.5	145 (polyn)[e]	
compound[b]				250 (dec)[c]	

[a] Two values for each parameter were provided due to two crystallographically independent molecules in the cell ($Z' = 2$). [b] Reference 19. [c] Decomposition temperature. [d] A mixture of forms II and II′ was used. [e] Polymerization temperature.

polymorphs are brought from the different circumstances around the reactive butadiyne units of **1**, as previously reported.[25a] Butadiyne contained [14]DBA is an attractive monomer for topochemical polymerization, as demonstrated by Vollhardt, Youngs, and co-workers.[19] For successful polymerization, specific orientations of the butadiyne moieties are required.[31] The present systems, however, did not meet the condition, judging from the geometrical parameters of the butadiyne: stacking distance of butadiynes (d), a neighboring $C_1 \cdots C_4$ distance of the 1,3-butadiyne moieties ($R_{1,4}$), and the angle between the molecular and stacking axis (γ), as shown in Table 1. [14]DBAs in forms I, II, and II′ are stacked with d values of 8.92–10.13 Å, while those in forms III and IV have d values of 3.87 and 3.81 Å. For all cases, the $R_{1,4}$ value is too long for the reaction. Indeed, insoluble black materials yielded after thermal decomposition showed no significant PXRD pattern, indicating disappearance of the stereoregular structure.

FT-IR Spectroscopy of Forms I–IV. In Figure 5a, observed FT-IR spectra of the polymorphs are shown. The bands of the C=O stretching for forms I, II/II′, III, and IV appeared at 1716, 1722, 1729, and 1726 cm^{-1}, respectively. However, no significant correlation was observed between the vibration wavenumbers and CH/O interaction distances or geometries. The C=C stretching region, on the other hand, shows clear differences between the spectra of forms I–III and that of form IV. The weak but unambiguous bands at 1544 and 1335 cm^{-1} are only present in the spectrum of form IV. Additionally, the band of form IV at 1402 cm^{-1} is weaker than those of the others. These bands characteristic for form IV are well reproduced in the theoretical spectrum calculated for the *hor-ver* conformer but not for the *ver-ver* one (Figure 5b). The bands at 1335 and 1402 cm^{-1} are attributed to the asymmetric C=C stretching vibration of the two benzene rings bearing the ester, with accompanying the in-plane C–H bending, while that at 1544 cm^{-1} to the symmetrical C=C stretching vibration of the three aromatic rings with accompanying the in-plane C–H bending (Figure S5 of the Supporting Information). These results demonstrated that the observed IR spectra of the polymorphs clearly reflect conformations of the molecules.

Fluorescence Properties of Forms I–IV. Compared with the fluorescence spectrum of **1** in solution ($\lambda_{max} = 400$ nm, $\phi_F = 0.40$, $\tau = 10.4$ ns) (Figures S1 and S2 of the Supporting Information), those of the polymorphs present in the lower energy region depend slightly on the polymorphic supramolecular structures

interactions: namely, the CH/O interaction with the methoxy group (S-1) or phenyl group (S-2), the branched interactions involving the methoxy and phenyl groups (B-1), and the complement interaction (C-1) as shown in Scheme 2. Tolerance of methyl ester groups for CH/O interaction, i.e. the versatile conformations and interaction ways, as well as the shape of the annulene core, enabled the molecules to pack into diverse arrangements.

Thermal Reactivity of Forms I–IV. To investigate the thermal behavior of the polymorphs, the obtained crystals were subjected to differential scanning calorimetry (DSC) analysis. In the following analyses, a mixture of forms II and II′ (II/II′) was used because of a separation problem. As shown in Figure S4 of the Supporting Information, the polymorphs showed no peaks ascribable to structural exchanges among the polymorphs or melting points. Therefore, the relative stability of each polymorph was not estimated, though the crystal density implies that the forms are stable in the order III (1.385 g cm^{-3} at 100 K), IV (1.375 g cm^{-3} at 100 K), I (1.331 g cm^{-3} at 213 K and 1.359 g cm^{-3} at 100 K; see the Supporting Information), II (1.349 g cm^{-3} at 100 K) $\sim$ II′ (1.328 g cm^{-3} at 213 K). On the other hand, forms I, II/II′, III, and IV show irreversible exothermic peaks at 254, 252, 240, and 245 °C with $\Delta H°$ values of 290–360 kJ/mol (Table 1). These temperature differences among the

5492

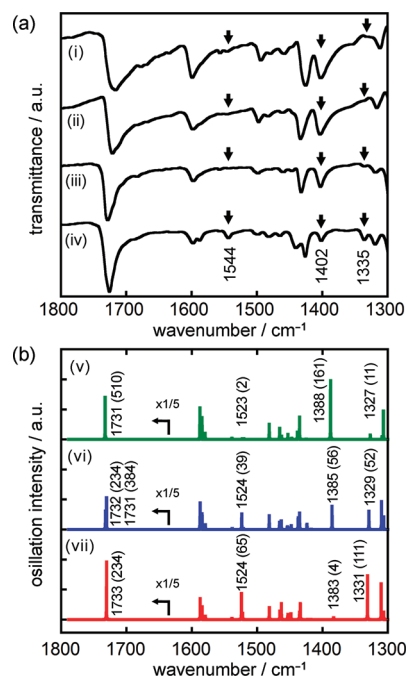dx.doi.org/10.1021/cg201075z |*Cryst. Growth Des.* 2011, 11, 5488–5497

Figure 5. Experimental and theoretical IR spectra of [14]DBA (**1**). (a) Experimental IR spectra of the polymorphs: forms I (i), II (ii), III (iii), and IV (iv). (b) Theoretical IR spectra of the conformers of [14]DBA (**1**): the *ver-ver* (v), *hor-ver* (vi), and *hor-hor* (vii) conformers. The oscillation intensities of selected peaks are listed in the parentheses.
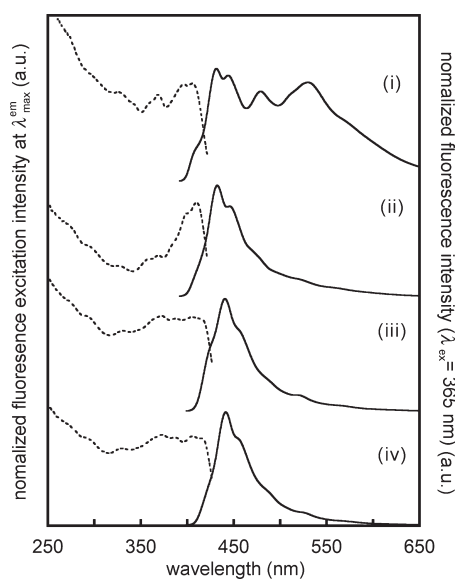

Figure 6. Normalized fluorescence (solid line) and excitation (dotted line) spectra of (i) forms I (G-rich), (ii) II, (iii) III, and (iv) IV.
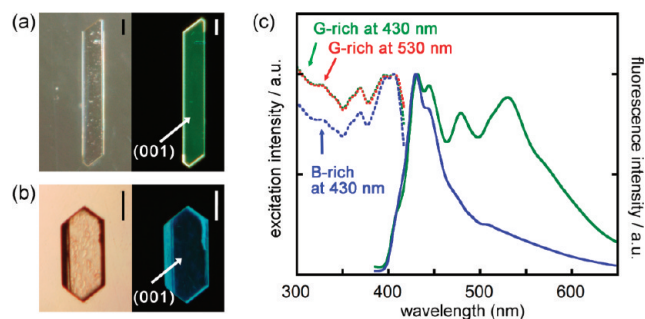

Figure 7. Photographs of two representative crystals of form I exhibiting (a) green and (b) blue fluorescence colors under UV light with wavelengths of 365 nm (right) and ambient light (left). Scale bars 200 μm. (c) Normalized fluorescence (solid line) and excitation (dotted line) spectra of the G-rich (green) and B-rich (blue) crystalline bulks. The excitation spectrum of the G-rich crystal at 430 nm (dotted green line) and that at 530 nm (dotted red line) show the same spectral profile.
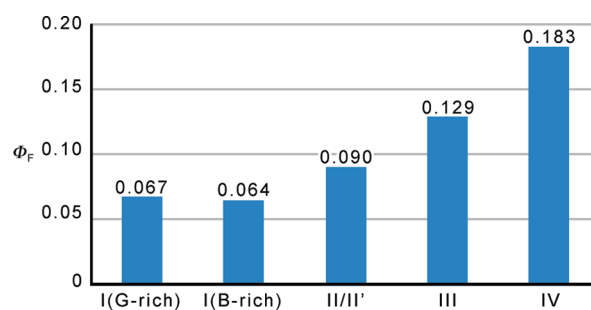

Figure 8. Fluorescence quantum yield of the polymorphic crystals: forms I(G-rich), I(B-rich), II/II′, III, and IV.

It is noteworthy that only form I exhibits a significant emission band at around 530 nm, as shown in Figure 6i. At first, we anticipated that the band was attributed to a new excited state with a low energy level due to species such as an excited dimer and oligomers specifically generated in form I. Later, however, we realized that the intensity of the band depended on the crystallization batches of form I. This observation cannot be explained by the excimer emission. As shown in Figure 7a and b, two crystals, both of which have the form I structure and explore the (1 0 0) face, exhibit either green or blue fluorescence. When these crystals are dissolved in a solvent, the resultant solutions show exactly the same UV−vis, fluorescence, and excitation spectra (Figure S6 of the Supporting Information). On the other hand, the crystalline bulk of form I with a green-rich fluorescence color [form I(G-rich)] obviously showed an emission band at around 530 nm, despite its excitation spectrum similar with that of the blue-rich crystal [form I(B-rich)], as shown in Figure 7c. Furthermore, the excitation spectrum of form I(G-rich) at 530 nm also shows good agreement with that at 430 nm, indicating that energy transfer occurs in the crystals.

To understand the optical properties of the polymorphs in more detail, the fluorescence quantum yield (Φ_F) and lifetime (τ) were determined for forms II/II′, III, and IV, as well as for form I(B-rich) and form I(G-rich). As shown in Figure 8, the Φ_F value is strongly dependent on the polymorphs: The Φ_F values are increasing in the order forms I, II/II′, III, and IV, and that of form IV is three times larger than that of form I. Usually, it is

(Figure 6). Forms I and II/II′ show a fluorescence maximum wavelength (λ_{max}^{em}) at 431 and 432 nm, respectively. Forms III and IV do at 441 and 440 nm, respectively, which are red-shifted by 10 nm compared with those of the formers. These results agree with the fact that the molecules in forms III and IV stack with larger π-planes overlap than those in forms I, II, and II′, although the structure-dependent difference is much smaller than our expectation.

Table 2. Fluorescence Lifetimes for Forms I–IV

form	λ_{max}^{em} (nm)	τ at $\lambda_{max}^{em\ b}$ (ns)	τ at lower energy region^{b,c} (ns)
I	431	0.58 ± 0.03(0.36)	0.75 ± 0.02(−0.08)^d
(G-rich)		1.85 ± 0.04(0.51)	4.66 ± 0.39(0.27)
		5.45 ± 0.10(0.13)	7.21 ± 0.04(0.81)
I	431	0.60 ± 0.06(0.13)	0.39 ± 0.04(−0.03)^d
(B-rich)		2.22 ± 0.05(0.59)	3.73 ± 0.09(0.47)
		5.20 ± 0.06(0.28)	8.12 ± 0.04(0.56)
II/II$'^a$	432	0.79 ± 0.06(0.09)	1.53 ± 0.15(−0.05)^d
		4.05 ± 0.25(0.44)	6.47 ± 0.11(0.83)
		10.1 ± 0.1(0.47)	13.4 ± 0.1(0.22)
III	441	2.20 ± 0.07(0.35)	4.00 ± 0.05(0.50)
		4.99 ± 0.03(0.65)	9.64 ± 0.05(0.50)
IV	440	3.17 ± 0.07(0.30)	4.42 ± 0.08(0.38)
		7.73 ± 0.03(0.70)	9.66 ± 0.04(0.62)

^{a} Forms II and II′ were measured as a mixture. ^{b} χ^2 values for forms I(B-rich), I(G-rich), II/II′, III, and IV are 1.167, 1.026, 1.232, 1.320, and 1.150 at 440 nm and 1.241, 1.038, 1.391, 1.216, and 1.112 at 540 nm. Relative amplitudes are shown in the parentheses. ^{c} The value was determined at 530 nm for forms I and II/II′ and 520 nm for III and IV. ^{d} A negative sign of the amplitude indicates that energy transfer occurs.

recognized that stacking of a π-molecule with a large π-overlap decreases the Φ_F value. In the present system, however, the trend is not in agreement with this idea. Probably these Φ_F values are given on subtle balances among the π-overlap degree and other causes, such as (1) loose molecular packing, which promotes nonradiative vibrational deactivation of the excitation state,[32,33] and (2) the distorted DBA ring from the planar conformation, which also has an influence on the rate of nonradiative deactivation.[34]

Time dependent fluorescence decay of the polymorphs was measured to determine fluorescence lifetimes at ca. 430 nm and ca. 530 nm (Figures S7–S11 of the Supporting Information). Forms I and II/II′ exhibit triexponential fluorescence decays as shown in Table 2 ($\tau_1 < 1$ ns, $\tau_2 = 2$–4 ns, $\tau_3 = 5$–10 ns) at 430 nm and ($\tau_1 < 2$ ns, $\tau_2 = 4$–6 ns, $\tau_3 = 7$–13 ns) at 530 nm, while forms III and IV exhibit biexponential ones ($\tau_1 = 2$–3 ns, $\tau_2 = 5$–8 ns) at 440 nm and ($\tau_1 = 4$ ns, $\tau_2 = 10$ ns) at 520 nm. These indicate that several excited states are involved in the fluorescence process. It is important that form I(G-rich) shows the lifetimes within 10 ns, which is too short for that of excimer emission.[35] This indicates that the fluorescence band at 530 nm is brought not from the excimer state but from another excited state. Furthermore, form I(G-rich) has the lifetime with a negative signed amplitude at 530 nm ($\tau_1 = 0.75$ ns). The negative sign denotes delay of the fluorescence decay. The delay and the fact that forms I(B-rich) and I(G-rich) show almost the same Φ_F values (0.06) strongly indicate effective energy transfer inflowed from another excited state, probably from that possessing the τ value of 0.60 ns at 430 nm. This is consistent with the unique excitation spectra at 430 and 530 nm, as described above. The negative delay is also observed for form II/II′, indicating the presence of the defects in form II/II′, although the fluorescence band at around 530 nm was not observed.

On the basis of these results, we conclude that the broad band at around 530 nm originates not from a specific molecular arrangement of form I, such as excimer formation, but from structural defects. The defects prefer to present specifically in form I and, subsequently, in form II/II′ crystals.
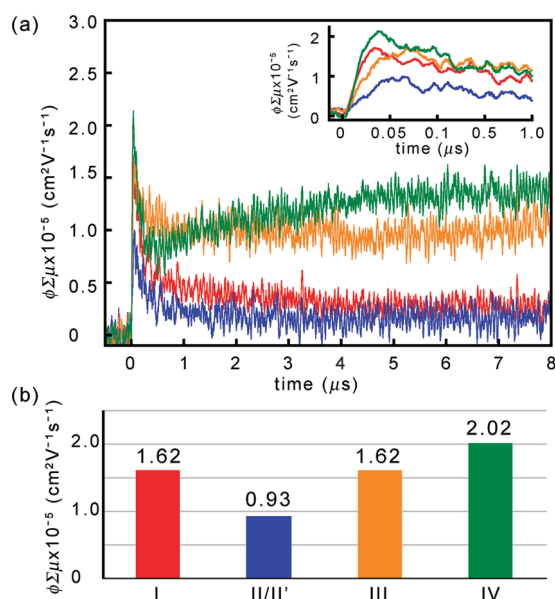

Figure 9. Photoconductivity of polymorphic crystals: forms I (red), II/II′ (blue), III (orange), and IV (green). (a) Transient curves. The inset shows the partially expanded transient curves. (b) Maximum values of the photoconductivity ($\phi\Sigma\mu$) of forms I (red), II/II′ (blue), III (orange), and IV (green).

Electrical Properties of the Polymorphs. To investigate structure-dependent charge carrier dynamics in the crystals of [14]DBA **1**, the obtained polymorphic crystals were subjected to flash photolysis time-resolved microwave conductivity (FP-TRMC) measurements.[36] The TRMC technique, which can predict the nanometer-scale mobility of charge carriers generated by laser pulse irradiation under a low oscillating microwave electric field, has been applied to assess the intrinsic mobility of π-conjugated polymers and π–π-stacked discotic materials,[36,37] because the peak-value is not significantly affected by chemical or physical defects in the material or the organic/metal-electrode interface. Irradiation of the laser flash brings rise and decay profiles of TRMC signals ($\phi\Sigma\mu$), where ϕ denotes the photocarrier generation yield and $\Sigma\mu$ the dose sum of the mobilities of the generated charge carriers; in the case of the DBA substituted by carboxyl groups or esters, the carrier is a hole.[17] In the present systems, the ϕ value was not determined because of the difficulty in spectroscopic evaluation of the crystals. Therefore, the $\phi\Sigma\mu$ transients were applied to compare the charge carrier dynamics of the polymorphs.

For crystals of forms I, III, and IV, the microwave electric field was applied for unisotropically aligned crystalline bulks, and the photoconductivity was measured along the b axis, which is corresponding to the columnar axis of the π-stacked [14]DBA molecules. On the other hand, for form II/II′, an isotropically laid crystalline powder was used for the measurement because of a technical problem caused by crystal size and shape.

Figure 9a shows the transient photoconductivities of the polymorphs observed by FP-TRMC. Surprisingly, the maximum values of $\phi\Sigma\mu$ for the polymorphs were significantly small (Figure 9b); even for forms III and IV (1.6×10^{-5} and 2.0×10^{-5} cm^2 V^{-1} s^{-1}, respectively), which have largely π-overlapped columnar structures, the value is 2 orders of magnitude less than that of the slipped stacked [12]DBA systems (2×10^{-3} cm^2 V^{-1} s^{-1}) we previously reported.[17] Comparison of the

5494

dx.doi.org/10.1021/cg201075z |*Cryst. Growth Des.* 2011, 11, 5488–5497

$\phi\Sigma\mu$ values among the polymorphs indicates that form IV shows slightly large conductivity, although they have quite similar values. The lifetime of the charge carrier, on the other hand, is significantly dependent on the molecular arrangements. Namely, in the crystals of forms III and IV, the charge carrier is still alive at 8 μs after its generation, while the carrier in the crystals of forms I and II/II′ was almost extinct at that time (Figure 9a). The observed fast decay in the latter crystals suggests that forms I and II/II′ contain a large number of trapping sites.[38] These results correspond with those of fluorescence lifetime measurements.

■ CONCLUSION

In this paper, we demonstrated that the octadehydrotribenzo-[14]annulene derivative with two methyl ester groups in non-centrosymmetric positions ([14]DBA, **1**) gave five polymorphic crystals successfully: forms I (plate, $P2_1/c$), II (block, $P2_1/c$), II′ (block $P\bar{1}$), III (needle, $P2_1/c$), and IV (needle, $C2/c$). This is the largest number for polymorphic crystals of the DBA family. These versatile forms were provided by conformational and interactional versatility of the methyl ester group: the present systems contain two conformers (*ver-ver* and *hor-ver*) and four kinds of CH/O interactions. DBA core shape also played a role to achieve versatile molecular arrangements. The properties of the polymorphs (thermal stability, IR absorption, fluorescence property, and charge carrier dynamics) were investigated. Such properties depend on the polymorphs. Furthermore, more fatally, structural defects have an influence on the optical and electrical properties. We demonstrated that the polymorphs exhibited structural defects depending on the magnitude of π-overlap of the DBA planes (I > II/II′ > III ~ IV), and the fluorescence and charge carrier properties were strongly affected by the defects. Particularly, form I shows a significant fluorescence band at 530 nm due to defects in the crystals.

The present molecular design to obtain polymorphic crystals of planar π-conjugated molecules is expected to contribute to the understanding not only of the relationships between structures and physical properties but also of the degree of molecular order in crystals, and to advanced design of DBA-based functional materials.

■ EXPERIMENTAL SECTION

X-ray Diffraction Measurements. Powder X-ray diffraction data were collected on a Rigaku RINT-2000 using graphite-monochromatized Cu Kα radiation (λ = 1.54187 Å) at room temperature. Single crystal diffraction: Diffraction data were collected on a Rigaku R-AXIS RAPID diffractometer with a 2-D area detector using graphite-monochromatized Cu Kα radiation (λ = 1.54187 Å) for forms I and II and by using the synchrotron radiation (λ = 0.7000 Å) at the BL38B1 in the SPring-8 with approval of JASRI (proposal nos. 2009B2115 and 2010A1427) for forms II, III, and IV. The cell refinements were performed with HKL2000 software[39] for forms II, III, and IV. Direct methods (SIR-2004) were used for the structure solution of all polymorphs.[40] All calculations were performed with the observed reflections [$I > 2\sigma(I)$] with the program CrystalStructure crystallographic software packages,[41] except for refinement, which was performed using SHELXL-97.[42] All non-hydrogen atoms, except for the case of form IV, were refined with anisotropic displacement parameters, and hydrogen atoms were placed in idealized

positions and refined as rigid atoms with the relative isotropic displacement parameters.

Fluorescence Measurements. Emission spectra in solid states were measured on a JASCO FP-6500 spectrofluorometer with an accessory and a cell for solid samples from JASCO. The fluorescence decay time and lifetime were obtained using HORIBA FluoroCube and the software (Data Station v.2.4 and DAS 6) supplied with the apparatus.

Charge Carrier Mobility Measurement. Nanosecond laser pulses from a Nd:YAG laser (third harmonic generation, THG (355 nm) from Spectra Physics, INDY, fwhm 5−8 ns) were used as excitation sources. The incident photon density of the laser was set at 1.4 × 10^{16} photons/cm^2/pulse. For time-resolved microwave conductivity (TRMC) measurements, the microwave frequency and power were set at ~9.1 GHz and 3 mW, respectively, so that the motion of the charge carriers was not disturbed by the low electric field of the microwaves. The TRMC signal picked up by a diode (rise time <1 ns) is monitored with a digital oscilloscope. All the above experiments were carried out at room temperature. The photoconductivity is given by the equation $\phi\Sigma\mu = (1/eAI_0F_{\text{light}})(\Delta P_r/P_r)$, where ϕ, $\Sigma\mu$, e, A, I_0, F_{light}, P_r, and ΔP_r denote photocarrier generation yield, the sum of the charge carrier mobilities, the unit charge of a single electron, the sensitivity factor (S^{-1} cm), the incident photon density of an excitation laser (photon cm^{-2}), the filling factor (cm^{-1}), and the reflected microwave power and its change, respectively.

Theoretical Study. The DFT calculations were performed with the Gaussian 03 program package.[43] The geometries of the conformers were optimized by using the B3LYP method in combination with the 6-31G* basis set. The theoretical IR spectra of the conformers were calculated for their optimized geometries. The wavelength of the resulting spectrum was scaled by 0.9614.[44]

Syntheses. Acyclic Tetrayne 4. 1,2-Bis(trimethylsilylethynyl)-benzene (768 mg, 2.84 mmol) and anhydrous K$_2$CO$_3$ (3.93 g, 28.4 mmol) in methanol/ether (51/13 mL) were stirred at room temperature for 1.5 h. The mixture was extracted with CH$_2$Cl$_2$ and washed with water and brine. The organic layer was dried over anhydrous MgSO$_4$ and concentrated in vacuo to yield **3** as a yellow oil. The oil **3** was added to a mixture of **2**[16] (2.24 g, 6.25 mmol), Pd(PPh$_3$)$_4$ (164 mg, 142 μmol), CuI (54.1 mg, 284 μmol), and ^{i}Pr$_2$NH (2.0 mL) in THF (25 mL). After it was stirred for 22 h at room temperature, the reaction mixture was concentrated in vacuo. The mixture was extracted with CH$_2$Cl$_2$ and washed with water and brine. The organic layer was dried over anhydrous MgSO$_4$ and concentrated in vacuo. Purification by column chromatography (silica gel, CH$_2$Cl$_2$) and preparative HPLC gave **4** (1.29 g, 78%) as a yellow solid. mp 130.5−133 °C, ^{1}H NMR (270 MHz, CDCl$_3$): δ 8.19 (d, J = 1.4 Hz, 2H, ArH), 7.92 (dd, J_1 = 1.6 Hz, J_2 = 8.1 Hz, 2H, ArH), 7.65−7.58 (m, 4H, ArH), 7.39−7.36 (m, 2H, ArH), 3.93 (s, 6H, OCH_3), 0.23 (s, 18H, SiCH_3) ppm. ^{13}C NMR (67.5 MHz, CDCl$_3$): δ 165.9, 133.4, 132.1, 132.1, 130.2, 129.6, 128.9, 128.6, 125.9, 125.6, 102.4, 100.0, 94.8, 91.9, 52.4, −0.1 ppm. HR-MS (FAB) m/z calcd for [M + H]$^+$ C$_{36}$H$_{35}$O$_4$Si$_2$ 587.2074, found 587.2088.

[14]DBA 1. A 1.0 M solution of TBAF in THF (0.29 mL) was added dropwise to a solution of **4** (171 mg, 0.291 mmol) in THF (8 mL) at room temperature. After it was stirred for 1 h, the mixture was extracted with CHCl$_3$ and washed with water and brine. The organic layer was dried over anhydrous MgSO$_4$ and concentrated in vacuo to yield a light brown solid. The resulting material was used for the following step without further

purification. A drop of the material obtained in the reaction above in pyridine (20 mL) was added into CuCl (289 mg, 2.91 mmol) in pyridine/methanol (150/150 mL). After it was stirred for 2 h at room temperature, the reaction mixture was concentrated in vacuo. The mixture was extracted with CHCl$_3$ and washed with water and brine. The organic layer was dried over anhydrous MgSO$_4$ and concentrated in vacuo. Purification by column chromatography (silica gel, CH$_2$Cl$_2$) gave **1** (88.7 mg, 69% for 2 steps) as a light yellow solid. ^{1}H NMR (270 MHz, CDCl$_3$): δ 8.25 (d, *J* = 1.4 Hz, 2H, Ar*H*), 8.12 (dd, *J*$_1$ = 1.8 Hz, *J*$_2$ = 8.1 Hz, 2H, Ar*H*), 7.93−7.89 (m, 4H, Ar*H*), 7.52−7.46 (m, 2H, Ar*H*), 3.96 (s, 6H, OC*H*$_3$) ppm. ^{13}C NMR (67.5 MHz, CDCl$_3$): δ 165.8, 136.4, 133.4, 133.1, 130.4, 129.5, 129.3, 128.6, 123.2, 122.8, 96.4, 92.7, 85.2, 80.8, 52.5 ppm. HR-MS (FAB) *m/z* calcd for [M]$^+$ C$_{30}$H$_{16}$O$_4$ 440.1049, found 440.1052.

■ ASSOCIATED CONTENT

⑤ Supporting Information. Optical properties of **1** in a solution, crystallization conditions, fluorescence decay profiles, PXRD patterns, theoretical IR vibration modes, DSC curves, ^{1}H and ^{13}C NMR spectra of new compounds, and X-ray crystallographic data for the five polymorphs. This material is available free of charge via the Internet at http://pubs.acs.org.

■ AUTHOR INFORMATION

Corresponding Author
*Telephone and fax: +81-6-6879-7406. E-mail: (I.H.) hisaki@mls.eng.osaka-u.ac.jp; (M.M.) miyata@mls.eng.osaka-u.ac.jp.

■ ACKNOWLEDGMENT

■ REFERENCES

(1) (a) Anthony, J. E. *Chem. Rev.* **2006**, *106*, 5028–5048. (b) Wu, J.; Pisula, W.; Müllen, K. *Chem. Rev.* **2007**, *107*, 718–747. (c) Hoeben, F. J. M.; Jonkheijm, P.; Meijer, E. W.; Schenning, A. P. H. J. *Chem. Rev.* **2005**, *105*, 1491–1546. (d) Kato, T.; Mizoshita, N.; Kishimoto, K. *Angew. Chem., Int. Ed.* **2006**, *45*, 38–68. (e) Würthner, F.; Kaiser, T. E.; Saha−Möller, C. R. *Angew. Chem., Int. Ed.* **2011**, *50*, 3376–3410.

(2) For reviews, see:(a) Bernstein, J.; Davey, R. J.; Henck, J.-O. *Angew. Chem., Int. Ed.* **1999**, *38*, 3440–3461. (b) Moulton, B.; Zaworotko, M. J. *Chem. Rev.* **2001**, *101*, 1629–1658.(c) Bernstein, J. *Polymorphism in Molecular Crystals*; Oxford University Press: New York, 2002. (d) Blagden, M.; Davey, R. J. *Cryst. Growth Des.* **2003**, *3*, 873–885. (e) Desiraju, G. R. *Angew. Chem., Int. Ed.* **2007**, *46*, 8342–8356. (f) *Making Crystals by Design*; Braga, D., Grepioni, F., Eds.; Wiley-VCH: Weinheim, 2007. (g) *Polymorphism: in the Pharmaceutical Industry*; Hifiker, R., Ed.; Wiley-VCH: Weinheim, 2007. (h) Mangin, D.; Puel, F.; Veesler, S. *Org. Process. Res. Dev.* **2009**, *13*, 1241–1253. (i) Kitamura, M. *CrystEngComm* **2009**, *11*, 949–964.

(3) (a) Mori, T. *Chem. Rev.* **2004**, *104*, 4947–4969. (b) Kobayashi, H.; Cui, H.; Kobayashi, A. *Chem. Rev.* **2004**, *104*, 5265–5288.

(4) Sorai, M.; Nakano, M.; Miyazaki, Y. *Chem. Rev.* **2006**, *106*, 976–1031.

(5) (a) Row, T. N. G. *Coord. Chem. Rev.* **1999**, *183*, 81–100. (b) Tanaka, K.; Toda, F. *Chem. Rev.* **2000**, *100*, 1025–1074. (c) Matsumoto, A. *Top. Curr. Chem.* **2005**, *254*, 263–305.

(6) Morimoto, M.; Kobatake, S.; Irie, M. *Chem.—Eur. J.* **2003**, *9*, 621–627.

(7) (a) Zhang, H.; Zhang, Z.; Ye, K.; Zhang, J.; Wang, Y. *Adv. Mater.* **2006**, *18*, 2369–2372. (b) Yago, T.; Tamaki, Y.; Furube, A.; Katoh, R. *Chem. Lett.* **2007**, *36*, 370–371. (c) Kohmoto, S.; Tsuyuki, R.; Masu, J.; Azumaya, I.; Kishikawa, K. *Tetrahedron Lett.* **2008**, *49*, 39–43. (d) Mutai, T.; Tomoda, H.; Ohkawa, T.; Yabe, Y.; Araki, K. *Angew. Chem., Int. Ed.* **2008**, *47*, 9522–9524. (e) Maeda, H.; Bando, Y.; Haketa, Y.; Honsho, Y.; Seki, S.; Nakajima, H.; Tohnai, N. *Chem.—Eur. J.* **2010**, *16*, 10994–11002. (f) Zhang, G.; Lu, J.; Sabat, M.; Fraser, C. L. *J. Am. Chem. Soc.* **2010**, *132*, 2160–2162.

(8) McCrone, W. C. *Polymorphism. In Physics and chemistry of the organic solid state*; Fox, D., Labes, M. M., Weissberger, A., Eds.; Wiley Interscience: New York, 1965; pp 725−767.

(9) Comprehensive reports for recent polymorphs, see:Brittain, H. G. *J. Pharm. Sci.* **2007**, *96*, 705–728. **2008**, *97*, 3611–3636. **2009**, *98*, 1617–1642. **2010**, *99*, 3648–3664.

(10) For conformational polymorphism, for example, see:(a) Jetti, R. K. R.; Boese, R.; Sarma, J. A. R. P.; Reddy, L. S.; Vishweshwar, P.; Desiraju, G. R. *Angew. Chem., Int. Ed.* **2003**, *42*, 1963–1967. (b) Bis, J. A.; Vishweshwar, P.; Middleton, R. A.; Zaworotko, M. *J. Cryst. Growth Des.* **2006**, *6*, 1048–1053. (c) Sokolov, A. N.; Swenson, D. C.; MacGillivray, L. R. *Proc. Natl. Acad. Sci.* **2008**, *105*, 1794–1797. (d) Dey, S. K.; Das, G. *Cryst. Growth Des.* **2010**, *10*, 754–760.

(11) For synthon polymorphism, for example, see:(a) Aakeröy, C. B.; Nieuwenhuyzen, M.; Price, S. L. *J. Am. Chem. Soc.* **1998**, *120*, 8986–8993. (b) Aakeröy, C. B.; Beatty, A. M.; Helfrich, B. A.; Nieuwenhuyzen, M. *Cryst. Growth Des.* **2003**, *3*, 159–165. (c) Roy, S.; Matzger, A. J. *Angew. Chem., Int. Ed.* **2009**, *48*, 8505–8508. (d) Li, J.; Bourne, S. A.; Caira, M. R. *Chem. Commun.* **2011**, *47*, 1530–1532.

(12) Yu, L. *Acc. Chem. Res.* **2010**, *43*, 1257–1266 and refs therein.

(13) Nangia, A. *Acc. Chem. Res.* **2008**, *41*, 595–604 and refs therein.

(14) (a) Walsh, R. D. B.; Bradner, M. W.; Fleischman, S.; Morales, L. A.; Moulton, B.; Rodriguez-Hornedo, N.; Zaworotko, M. J. *Chem. Commun.* **2003**, *2*, 186–187. (b) Porter, W. W., III; Elie, S. C.; Matzger, A. J. *Cryst. Growth Des.* **2008**, *8*, 14–16.

(15) Polymorphs of some large π-conjugated systems, such as copper phthalocyanine and pentacene, have been investigated, for example, see ref 2c and the following literature: (a)Mattheus, C. C.; Dros, A. B.; Baas, J.; Oostergetel, G. T.; Meetsma, A.; de Boer, J. L.; Palstra, T. T. M. *Synth. Met.* **2003**, *138*, 475–481.

(16) (a) Cornil, J.; Lemaur, V.; Calbert, J.-P.; Brédas, J.-L. *Adv. Mater.* **2002**, *14*, 726–729. (b) Lemaur, V.; da Silva Filho, D. A.; Coropceanu, V.; Lehmann, M.; Geerts, Y.; Piris, J.; Debije, M. G.; van de Craats, A. M.; Senthilkumar, K.; A Siebbeles, L. D.; Warman, J. M.; Brédas, J.-L.; Cornil, J. *J. Am. Chem. Soc.* **2004**, *126*, 3271–3279. (c) Marcon, V.; Breiby, D. W.; Pisula, W.; Dahl, J.; Kirkpatrick, J.; Patwardhan, S.; Grozema, F.; Andrienko, D. *J. Am. Chem. Soc.* **2009**, *131*, 11426–11432. (d) Feng, X.; Marcon, V.; Pisula, W.; Hansen, M. R.; Kirkpatrick, J.; Grozema, F.; Andrienko, D.; Kremer, K.; Müllen, K. *Nat. Mater.* **2009**, *8*, 421–426.

(17) Hisaki, I.; Sakamoto, Y.; Shigemitsu, H.; Tohnai, N.; Miyata, M.; Seki, S.; Saeki, A.; Tagawa, S. *Chem.—Eur. J.* **2008**, *14*, 4178–4187.

(18) Reviews for dehydrobenzoannulenes, see:(a) Bunz, U. H. F.; Rubin, Y.; Tobe, Y. *Chem. Soc. Rev.* **1999**, *28*, 107–119. (b) Youngs, W. J.; Tessier, C. A.; Bradshaw, J. D. *Chem. Rev.* **1999**, *99*, 3153–3177.(c) Jones, C. S.; O'Connor, M. J.; Haley, M. M. In *Acetylene Chemistry*; Diederich, F., Stang, P. J., Tykwinski, R. R., Eds.; Wiley-VCH: Weinheim, 2005; pp 303−385. (d) Hisaki, I.; Sonoda, M.; Tobe, Y. *Eur. J. Org. Chem.* **2006**, 833–847. (e) Spitler, E. L.; Johnson, C. A., II; Haley, M. M. *Chem. Rev.* **2006**, *106*, 5344–5386.(f) Sadowy, A. L.; Tykwinski, R. R. In

Modern Supramolecular Chemistry; Diederich, F., Stang, P. J., Tykwinski, R. R., Eds.; Wiley-VCH: Weinheim, 2008; pp 185−231.

(19) Baldwin, K. P.; Matzger, A. J.; Scheiman, D. A.; Tessier, C. A.; Vollhardt, K. P. C.; Youngs, W. J. *Synlett* **1995**, 1215–1218.

(20) (a) Boydston, A. J.; Haley, M. M. *Org. Lett.* **2001**, 3, 3599–3601. (b) Boydston, A. J.; Haley, M. M.; Williams, R. V.; Armantrout, J. R. *J. Org. Chem.* **2002**, 67, 8812–8819.

(21) (a) Kimball, D. B.; Haley, M. M.; Mitchell, R. H.; Ward, T. R. *Org. Lett.* **2001**, 3, 1709–1711. (b) Kimball, D. B.; Haley, M. M.; Mitchell, R. H.; Ward, T. R.; Bandyopadhyay, S.; Williams, R. V.; Armantrout, J. R. *J. Org. Chem.* **2002**, 67, 8798–8811.

(22) (a) Hinrichs, H.; Fischer, A. K.; Jones, P. G.; Hopf, H.; Haley, M. M. *Org. Lett.* **2005**, 7, 3783–3795. (b) Hinrichs, H.; Boydston, A. J.; Jones, P. G.; Hess, K.; Herges, R.; Haley, M. M.; Hopf, H. *Chem.—Eur. J.* **2006**, 12, 7103–7115.

(23) Marsden, J. A.; Miller, J. J.; Shirtdiff, L. D.; Haley, M. M. *J. Am. Chem. Soc.* **2005**, 127, 2464–2476.

(24) Takeda, T.; Fix, A. G.; Haley, M. M. *Org. Lett.* **2010**, 12, 3824–3827.

(25) (a) Hisaki, I.; Sakamoto, Y.; Shigemitsu, H.; Tohnai, N.; Miyata, M. *Cryst. Growth Des.* **2009**, 9, 414–420. (b) Hisaki, I.; Shigemitsu, H.; Sakamoto, Y.; Hasegawa, Y.; Okajima, Y.; Nakano, K.; Tohnai, N.; Miyata, M. *Angew. Chem., Int. Ed.* **2009**, 48, 5465–5469.

(26) (a) Desiraju, G. R.; Steiner, T. *The Weak Hydrogen Bond in Structural Chemistry and Biology*; Oxford University Press: Oxford, 1999. (b) Steiner, T. *Angew. Chem., Int. Ed.* **2002**, 41, 48–76. (c) Desiraju, G. R. *Chem. Commun.* **2005**, 2995–3001.

(27) Crystal data for form I: $C_{30}H_{16}O_4$, M_w = 440.45, a = 11.5094(2), b = 8.92224(16), c = 21.9131(4) Å, α = 90, β = 102.4710(9), γ = 90°, V = 2197.16(7) Å^3, T = 213 K, monoclinic, space group $P2_1/c$ (No. 14), Z = 4, ρ_{calcd} = 1.331 g cm^{-3}, 3969 unique reflections, the final $R1$ and $wR2$ values 0.051 ($I > 2.0\sigma(I)$) and 0.144 (all data), respectively.Crystal data for form II: $C_{30}H_{16}O_4$, M_w = 440.45, a = 10.1300(1), b = 13.8586(2), c = 16.1692(3) Å, α = 90, β = 107.1536(6), γ = 90°, V = 2168.98(6) Å^3, T = 100 K, monoclinic, space group $P2_1/c$ (No. 14), Z = 4, ρ_{calcd} = 1.349 g cm^{-3}, 4550 unique reflections, the final $R1$ and $wR2$ values 0.062 ($I > 2.0\sigma(I)$) and 0.178 (all data), respectively. Crystal data for form II′: $(C_{30}H_{16}O_4)_2$, M_w = 880.91, a = 9.88125(18), b = 10.12115(18), c = 22.1855(4) Å, α = 95.3050(9), β = 93.7500(9), γ = 91.7710(10)°, V = 2203.01(7) Å^3, T = 213 K, triclinic, space group $P\bar{1}$ (No. 2), Z = 2, ρ_{calcd} = 1.328 g cm^{-3}, 7759 unique reflections, the final $R1$ and $wR2$ values 0.065 ($I > 2.0\sigma(I)$) and 0.158 (all data), respectively. Crystal data for form III: $(C_{30}H_{16}O_4)$, M_w = 440.45, a = 25.991(4), b = 3.8710(3), c = 21.352(4) Å, α = 90, β = 100.522(7), γ = 90°, V = 2112.1(5) Å^3, T = 100 K, monoclinic, space group $P2_1/c$ (No. 14), Z = 4, ρ_{calcd} = 1.385 g cm^{-3}, 2291 unique reflections, the final $R1$ and $wR2$ values 0.168 ($I > 2.0\sigma(I)$) and 0.454 (all data), respectively.Crystal data for form IV: $C_{30}H_{16}O_4$, M_w = 440.45, a = 46.1390(8), b = 3.85580(10), c = 28.7157(7) Å, α = 90, β = 123.6138(9), γ = 90°, V = 4254.38(17) Å^3, T = 100 K, monoclinic, space group $C2/c$ (No. 15), Z = 8, ρ_{calcd} = 1.375 g cm^{-3}, 4693 unique reflections, the final $R1$ and $wR2$ values 0.070 ($I > 2.0\sigma(I)$) and 0.203 (all data), respectively.CCDC 814048(form I), 814049-(form II), 831522(form II′), 814050(form III), and 814051 (form IV) contain the supplementary crystallographic data for this paper. These data can be obtained free of charge from The Cambridge Crystallographic Data Centre via www.ccdc.cam.ac.uk/data_request/cif.

(28) The crystal structure of form III was resolved isotropically because some anisotropic displacement parameters were nonpositive due to the high mosicity caused by the plasticity of the thin needle crystals. The resultant structure, however, is reliable because the maximum laest-square shift error converged to zero.

(29) Hierarchical interpretation of organic crystals, see:(a) Tanaka, A.; Inoue, K.; Hisaki, I.; Tohnai, N.; Miyata, M.; Matsumoto, A. *Angew. Chem., Int. Ed.* **2006**, 45, 4142–4145. (b) Miyata, M.; Tohnai, N.; Hisaki, I. *Acc. Chem. Res.* **2007**, 40, 694–702.

(30) The crystal of form II′ has two crystallographically independent molecules. However, Figure 3c shows the CH/O interactions for only one of them.

(31) Wegner, G. Z. *Naturforsch., B: Chem. Sci.* **1969**, 24, 824–832.

(32) Scott, J. L.; Yamada, T.; Tanaka, K. *New J. Chem.* **2004**, 28, 447–450.

(33) (a) Mizobe, Y.; Ito, H.; Hisaki, I.; Miyata, M.; Hasegawa, Y.; Tohnai, N. *Chem. Commun.* **2006**, 2126–2128. (b) Hinoue, T.; Mizobe, Y.; Hisaki, I.; Miyata, M.; Tohnai, N. *Chem. Lett.* **2008**, 37, 642–643.

(34) Lai, R. Y.; Fleming, J. J.; Merner, B. L.; Vermeij, R. J.; Bodwell, G. J.; Bard, A. J. *J. Phys. Chem. A* **2004**, 108, 376–383.

(35) Stevens, B. *Nature* **1961**, 25, 725–727.

(36) (a) Seki, S.; Yoshida, Y.; Tagawa, S.; Asai, K.; Ishigure, K.; Furukawa, K.; Fujiki, M.; Matsumoto, M. *Philos. Mag. B* **1999**, 79, 1631–1645. (b) Grozema, F. C.; Siebbeles, L. D. A.; Warman, J. M.; Seki, S.; Tagawa, S.; Scherf, U. *Adv. Mater.* **2002**, 14, 228–231. (c) Saeki, A.; Seki, S.; Sunagawa, T.; Usida, K.; Tagawa, S. *Philos. Mag. B* **2006**, 86, 1261–1276. (d) Saeki, A.; Seki, S.; Takenobu, T.; Iwasa, Y.; Tagawa, S. *Adv. Mater.* **2008**, 20, 920–923.

(37) For recent examples, see:(a) Yamamoto, Y.; Fukushima, T.; Suna, Y.; Ishii, N.; Saeki, A.; Seki, S.; Tagawa, S.; Taniguchi, M.; Kawai, T.; Aida, T. *Science* **2006**, 314, 1761–1764. (b) Amaya, T.; Seki, S.; Moriuchi, T.; Nakamoto, K.; Nakata, T.; Sakane, H.; Saeki, A.; Tagawa, S.; Hirao, T. *J. Am. Chem. Soc.* **2009**, 131, 408–409. (c) Maeda, H.; Bando, Y.; Haketa, Y.; Honsho, Y.; Seki, S.; Nakajima, H.; Tohnai, N. *Chem.—Eur. J.* **2010**, 16, 10994–11002. (d) Sakurai, T.; Tashiro, K.; Honsho, Y.; Saeki, A.; Seki, S.; Osuka, A.; Muranaka, A.; Uchiyama, M.; Kim, J.; Ha, S.; Kato, K.; Takata, M.; Aida, T. *J. Am. Chem. Soc.* **2011**, 133, 6537–6540.

(38) Li, W.-S.; Yamamoto, Y.; Fukushima, T.; Saeki, A.; Seki, S.; Tagawa, S.; Masunaga, H.; Sasaki, S.; Takata, M.; Aida, T. *J. Am. Chem. Soc.* **2008**, 130, 8886–8887.

(39) Otwinowski, Z.; Minor, W. *Methods Enzymol.* **1997**, 276, 307–326.

(40) Altomare, A.; Burla, M.; Camalli, M.; Cascarano, G.; Giacovazzo, C.; Guagliardi, A.; Moliterni, A.; Polidori, G.; Spagna, R. *J. Appl. Crystallogr.* **1999**, 32, 115–119.

(41) *CrystalStructure ver 3.8*, Crystal Structure Analysis Package; Rigaku and Rigak Americas: The Woodlands, TX, 2000−2007.

(42) Sheldrick, G. M. *Acta Crystallogr., A* **2008**, 64, 112–122.

(43) *Gaussian 03*, Revision D.01; Frisch, M. J., et al. Gaussian, Inc.: Wallingford, CT, 2004.

(44) Scott, A. T.; Radom, L. *J. Phys. Chem.* **1996**, 100, 16502–16513.